Resistive Network Optimal Power Flow: Uniqueness and Algorithms

Chee Wei Tan, *Senior Member, IEEE*, Desmond W. H. Cai, *Student Member, IEEE* and Xin Lou

***Abstract*—The optimal power flow (OPF) problem minimizes the power loss in an electrical network by optimizing the voltage and power delivered at the network buses, and is a nonconvex problem that is generally hard to solve. By leveraging a recent development on the zero duality gap of OPF, we propose a second-order cone programming convex relaxation of the resistive network OPF, and study the uniqueness of the optimal solution using differential topology especially the Poincare–Hopf Index Theorem. We characterize the global uniqueness for different network topologies, e.g., line, radial and mesh networks. This serves as a starting point to design distributed local algorithms with global behaviors that have low complexity, computationally fast and can run under synchronous and asynchronous settings in practical power grids.**

I. Introduction

The Optimal Power Flow (OPF) problem is a classical nonlinear and nonconvex optimization problem that minimizes the power generation costs and transmission loss in a power network subject to physical constraints governed by Kirchhoff's and Ohm's law [1]–[3]. There is a huge body of work on solving the OPF since Carpentier's first formulation in 1962 [1]. To overcome the nonlinearity and nonconvexity, the majority of these work uses approximation methodologies to first simplify the OPF and then solve the approximated problem. For example, a popular approximation technique is the so-called DC OPF linearization that assumes a constant voltage and uses small angle approximation [4] and there are also other numerically efficient approximation methods [5]–[12]. It is a key challenge to find new optimization methodologies that can overcome the nonconvexity barrier to solve the OPF optimally and exactly, especially in a large-scale network.

Recent developments have shown that the OPF can be convexified using a reformulation-relaxation technique and semidefinite programming (SDP). We refer the readers to [14], [15] for an overview on this development that clarifies the relationships between various models of OPF and its convex relaxation. This is important because SDP is a convex optimization problem that can be efficiently solved [16]. In particular, the authors in [17], [18] showed that the Lagrange duality gap between the OPF problem and its convex dual can in fact be zero in a radial network, and this was numerically verified to be true for a number of practical IEEE power networks. Specifically, this SDP convex relaxation problem is in fact tight[1] when a certain load over-satisfaction condition is assumed [17], [19]. The load over-satisfaction condition[2] means that there is no lower bound on the real power consumption at each bus, and the power supplied to each bus in the network can be greater than their respective power demands.

There are other recent work on reformulation-relaxation techniques for the OPF. The author in [22] studied the convexification of the AC OPF using a branch flow model that utilizes a second-order cone programming (SOCP) relaxation for radial networks. The authors in [23] also proposed SOCP relaxation that are applicable to AC OPF based on the SDP relaxation work in [17], [18]. We note that, independent of the work in this paper and that in [23], an SOCP relaxation for the resistive network was proposed in a recent paper [24], where the authors studied an SOCP relaxation without the aforementioned load over-satisfaction assumption but requiring an infinite voltage upper bound, which is different from the work in this paper. In addition, the solution uniqueness of the AC OPF that uses the SDP convex relaxation has also been recently explored in [25].

In this paper, we leverage the developments in [17], [18] to further analyze the OPF problem in a purely resistive network (i.e., without phase angle, reactive power variables and reactance parameters). This kind of network can be practically important and promising in HVDC (high-voltage direct current) networks or microgrid clusters that integrate renewable energy sources (e.g., photovoltaic generator) that produce only real power. Indeed, studying the resistive network OPF and its algorithm design enables a deeper analysis of a problem with much simpler equations but still retaining

Manuscript received October 02, 2013; revised November 09, 2013, and February 14, 2014; accepted May 6, 2014. The work in this paper was partially supported by grants from the Research Grants Council of Hong Kong Project No. RGC CityU 122013, ARPA-E grant DE-AR0000226 and the National Science Council of Taiwan, R.O.C. grant paper published in 2014: NSC 103-3113-P-008-001.

C. W. Tan is with the College of Science and Engineering, City University of Hong Kong, Tat Chee Ave., Hong Kong and a visiting professor with the State Key Laboratory of Integrated Services Networks, Xidian University, China (email: cheewtan@cityu.edu.hk). D. W. H. Cai is with the Department of Electrical Engineering, California Institute of Technology, Pasadena, CA 91125 USA (e-mail: wccai@caltech.edu). X. Lou is with the College of Science and Engineering, City University of Hong Kong, Hong Kong.

[1]We say that a relaxation is tight when the relaxation has an optimal value that is equal to the global optimal value of the original nonconvex problem, and an optimal primal solution of the original problem can be obtained from an optimal primal solution of the relaxation.

[2]In this paper, we study the OPF with the load over-satisfaction assumption, which implies the zero-duality gap condition. It is however important to find out the extent to which this assumption is true and indeed there are recent work that study the limitations of this assumption (see, e.g., [20], [21]). It is interesting to find other new conditions under which the OPF has zero duality gap or can be convexified.

some of the important features of the general OPF, whose algorithm development can potentially be used for a more general OPF and the real applications [13]. We first propose an efficient SOCP relaxation of the resistive network OPF and prove its tightness under a monotonicity condition of the cost objective function. We then focus on the special case of transmission power loss minimization in the resistive network, and characterize the uniqueness of its optimal solutions for various network topologies. This has implications on how distributed algorithms can be designed to solve this loss minimization OPF problem. Our techniques and algorithms can also be extended to solve other kinds of OPF problem formulation. As an example, our distributed algorithms can be incorporated to solve a multi-period resistive network OPF with energy storage [26].

Our algorithm design differs from prior work in the vast literature, e.g., in [5]–[12], in the following aspects. We leverage the zero duality gap results in [17] and dual decomposition to design decentralized algorithms in which each bus (either the generator bus or the demand bus) performs a local information (e.g., voltages and powers) update and can also exchange the local information with its one-hop neighbors (either synchronously or asynchronously). The uniqueness characterization provides an interesting perspective on the optimal solution as well as the convergence proof of the local algorithms to the global optimal solution.

Overall, the contributions of the paper are as follows:

1) We propose a SOCP convex relaxation for the resistive network OPF and prove the tightness of this convex relaxation under mild conditions.
2) We characterize the uniqueness of the resistive network OPF solution using the Poincare-Hopf Index Theorem for different network topologies, and we illustrate our techniques using various illustrative examples and numerical evaluation.
3) We leverage the uniqueness property to solve the resistive network OPF problem using dual decomposition and iterative fixed-point analysis. Computationally fast convergent local algorithms with low complexity are proposed to compute the global optimal solution of the resistive network OPF in a distributed manner under both synchronous and asynchronous settings.

II. System Model and Problem Formulation

We consider a resistive power network with a set of buses $\mathcal{N} = \{1, 2, \ldots, N\}$ and a set of transmission lines $\mathcal{E} \subseteq \mathcal{N} \times \mathcal{N}$. We model the power flow in the network using the bus injection model that focuses on the voltage and the power injection at each bus of the network. We assume that each bus is either a generation bus or a demand bus. A demand bus i can model the aggregate of users (loads) in a power network. For each bus i, we use Ω_i to represent the set of buses connecting to bus i and $|\Omega_i| \geq 1$. Moreover, we assume that the line admittance satisfies $Y_{ij} = Y_{ji} \in \mathbb{R}_+$, if $(i,j) \in \mathcal{E}$; and $Y_{ij} = Y_{ji} = 0$, otherwise. In a purely resistive power network, the admittance matrix $\mathbf{Y}$ is given by $\mathbf{Y} = \mathbf{G}$, where $\mathbf{G}$ is the system conductance matrix. We assume that the graph of the power system is fully connected, i.e., there exists a path between every two buses of the network. We use $\mathbf{V}$ and $\mathbf{I}$ to denote the voltage magnitude vector $(V_i)_{i\in\mathcal{N}}$ and current magnitude vector $(I_i)_{i\in\mathcal{N}}$ respectively.

We consider nodal power and voltage constraints given by $V_i I_i \leq \bar{p}_i$ and $V_i \in [\underline{V}_i, \overline{V}_i]$, $\forall i \in \mathcal{N}$ respectively. If bus i is a generation bus, then $\bar{p}_i$ represents the generator capacity and $\bar{p}_i > 0$. If bus i is a demand bus, then $\bar{p}_j < 0$ and this constraint corresponds to the minimum demand that has to be satisfied at bus i. We assume that demand can be over-satisfied, which is a practical assumption when there are power storage devices available at the demand buses. Therefore, a demand bus i not only absorbs $|\overline{p}_i|$ amount of power, but it also absorbs additional power to charge the power storage device attached to it. Moreover, for each line $(i,j) \in \mathcal{E}$, we impose the line capacity constraint $G_{ij}(V_i - V_j)^2 \leq c_{ij}$. Then, the resistive network OPF can be formulated as minimizing an objective function $f(\mathbf{I}, \mathbf{V})$ (e.g., generation cost or transmission loss) over the resistive network subject to bus and line constraints:

$$\begin{array}{ll} \text{minimize} & f(\mathbf{I}, \mathbf{V}) \\ \text{subject to} & I_i V_i \leq \bar{p}_i \ \ \forall i \in \mathcal{N}, \\ & \underline{V}_i \leq V_i \leq \overline{V}_i \ \ \forall i \in \mathcal{N}, \\ & G_{ij}(V_i - V_j)^2 \leq c_{ij} \ \ \forall (i,j) \in \mathcal{E}, \\ \text{variables:} & V_i, I_i, i \in \mathcal{N}. \end{array} \tag{1}$$

By Ohm's Law and Kirchhoff's current law, we have $\mathbf{I} = \mathbf{G}\mathbf{V}$, i.e.,

$$\begin{pmatrix} I_1 \\ I_2 \\ \vdots \\ I_N \end{pmatrix} = \begin{pmatrix} \sum\limits_{j\in\Omega_1} G_{1j} & \cdots & -G_{1N} \\ -G_{21} & \cdots & -G_{2N} \\ \vdots & \ddots & \vdots \\ -G_{N1} & \cdots & \sum\limits_{j\in\Omega_N} G_{Nj} \end{pmatrix} \begin{pmatrix} V_1 \\ V_2 \\ \vdots \\ V_N \end{pmatrix}. \tag{2}$$

Substituting the above relationship between $\mathbf{G}$ and $\mathbf{I}$ into (1), the optimal power flow problem in (1) is equivalent to the following optimization problem with quadratic constraints:

$$\begin{array}{ll} \text{minimize} & f(\mathbf{V}) \\ \text{subject to} & \mathbf{V}^T \mathbf{G}_i \mathbf{V} \leq \overline{p}_i \ \ \forall i \in \mathcal{N}, \\ & \underline{\mathbf{V}} \leq \mathbf{V} \leq \overline{\mathbf{V}}, \\ & \mathbf{V}^T \mathbf{G}_{ij} \mathbf{V} \leq c_{ij} \ \ \forall (i,j) \in \mathcal{E}, \\ \text{variables:} & \mathbf{V}, \end{array} \tag{3}$$

where $\mathbf{G}_i = \frac{1}{2}(\mathbf{E}_i \mathbf{G} + \mathbf{G}\mathbf{E}_i)$ and $\mathbf{G}_{ij} = G_{ij}(\mathbf{e}_i - \mathbf{e}_j)(\mathbf{e}_i - \mathbf{e}_j)^T$, where $\mathbf{e}_i$ is the standard basis vector in $\mathbb{R}^n$ and $\mathbf{E}_i = \mathbf{e}_i \mathbf{e}_i^T \in \mathbb{R}^{n\times n}$ [17]. Let the optimal solution of (3) be $\mathbf{V}^*$. Since (3) is nonconvex, it is generally hard to solve for $\mathbf{V}^*$.

III. Second-Order Cone Programming Convex Relaxation

In this section, we propose a SOCP convex relaxation of (3), which is in fact tight under mild conditions on the objective function $f(\mathbf{V})$. Let us first introduce the auxiliary variables $W_{ii} = V_i^2$, $\forall i \in \mathcal{N}$ and $W_{ij} = V_i V_j$ $\forall (i,j) \in \mathcal{E}$. We shall also use the nonnegative matrix $\mathbf{W}$ to represent $(W_{ii})_{i\in\mathcal{N}}$

and $(W_{ij})_{(i,j)\in\mathcal{E}}$. We rewrite the objective function $f(\mathbf{V})$ in terms of the auxiliary variables to obtain $\hat{f}(\mathbf{W})$, so that (3) is equivalent to the following optimization problem:

$$\begin{array}{ll} \text{minimize} & \hat{f}(\mathbf{W}) \\ \text{subject to} & \sum\limits_{j\in\Omega_i} G_{ij}(W_{ii}-W_{ij}) \le \bar{p}_i \ \ \forall i \in \mathcal{N}, \\ & \underline{V}_i^2 \le W_{ii} \le \overline{V}_i^2 \ \ \forall i \in \mathcal{N}, \\ & G_{ij}(W_{ii}+W_{jj}-2W_{ij}) \le c_{ij} \ \ \forall (i,j) \in \mathcal{E}, \\ & W_{ii}W_{jj} = W_{ij}^2 \ \ \forall (i,j) \in \mathcal{E}, \\ & W_{ij} \ge 0, \ W_{ji} \ge 0 \ \ \forall (i,j) \in \mathcal{E}, \\ \text{variables:} & \mathbf{W}. \end{array} \tag{4}$$

Let the optimal solution of (4) be $\mathbf{W}^*$. Now, observe that all the constraints in (4) are convex in $\mathbf{W}$ except for the equality constraints $W_{ii}W_{jj} = W_{ij}^2 \ \ \forall (i,j) \in \mathcal{E}$. We consider relaxing these nonconvex constraints into the following inequality constraints:

$$W_{ii}W_{jj} \ge W_{ij}^2 \ \ \forall (i,j) \in \mathcal{E}, \tag{5}$$

which are equivalent to the following SOCP constraints:

$$\left|\left| \begin{array}{c} 2W_{ij} \\ W_{ii}-W_{jj} \end{array} \right|\right|_2 \le W_{ii}+W_{jj} \ \ \forall (i,j) \in \mathcal{E}. \tag{6}$$

Lemma 1: Suppose that $\hat{f}(\mathbf{W})$ is monotonically decreasing in $W_{ij}, \forall (i,j) \in \mathcal{E}$. Then, the relaxation of the resistive network OPF in (4) with SOCP constraints (6) is tight, and furthermore $\mathbf{W}^* = \mathbf{V}^*\mathbf{V}^{*T}$.

Proof: To prove the tightness of the SOCP relaxation, we show that there exists an optimal solution such that the constraints (5) are active, i.e., the inequalities become strictly equalities. Suppose that $\mathbf{W}^*$ is an optimal solution of the relaxed problem and there exists a line $(\ell_1, \ell_2) \in \mathcal{E}$ such that the constraint $W^*_{\ell 1 \ell 1} W^*_{\ell 2 \ell 2} \ge W^{*2}_{\ell_1 \ell_2}$ is inactive, i.e., a strict inequality. Since $\hat{f}(\mathbf{W})$ is decreasing in $W_{ij}, \forall (i,j) \in \mathcal{E}$, we can choose some $\hat{\mathbf{W}}$ such that $W^*_{\ell_1\ell_1} W^*_{\ell_2\ell_2} = \hat{W}^2_{\ell_1\ell_2} = W^{*2}_{\ell_1\ell_2} + \epsilon > W^{*2}_{\ell_1\ell_2}$ holds. Since $G_{ij} > 0, \mathbf{W} = \hat{\mathbf{W}}$ is feasible and gives a smaller objective value (contradicting the fact that $\mathbf{W}^*$ is optimal), it is also an optimal solution. ■

Remark 1: If $\hat{f}(\mathbf{W})$ is convex, then the SOCP relaxation of (4) is also convex and its duality gap is zero under mild conditions (Slater's conditions being satisfied) [16]. In addition, the SOCP relaxation of (4) can be solved by interior-point methods that have a much better worst case complexity than their SDP counterparts [16], and there are widely-available standard optimization packages (e.g., see [27]) that can solve SOCP efficiently.

In fact, observe that the transmission loss minimization satisfies the condition imposed on the objective function in Lemma 1 since, in the transmission loss minimization setting, we consider a quadratic objective function $f(\mathbf{V}) = \mathbf{V}^T\mathbf{G}\mathbf{V}$ (making $\hat{f}(\mathbf{W})$ linearly decreasing in W_{ij}). In the following, for simplicity and clarity, we shall focus on this objective function $f(\mathbf{V}) = \mathbf{V}^T\mathbf{G}\mathbf{V}$, and study the uniqueness of the optimal solution in (3) with ramification on the design of distributed algorithms to solve (3).

IV. Uniqueness Characterization

In this section, we study the uniqueness of the solution to (3). The uniqueness characterization of (3) has implications on how local algorithms with low complexity can be designed to solve (3) (see Section V). Our approach is to leverage the zero duality gap property in (3) and the Poincare-Hopf Index Theorem in [28], [29] together with the nonnegativity associated with the variables and problem parameters of (3).

We first use the Lagrange dual decomposition to relax (3). Define the following partial Lagrangian function:

$$\begin{aligned} L(\mathbf{V}, \{\boldsymbol{\lambda}, \boldsymbol{\mu}\}) \doteq & \sum_{(i,j)\in\mathcal{E}} (\lambda_i + 1) G_{ij} V_i (V_i - V_j) - \sum_{i\in\mathcal{N}} \lambda_i \overline{p}_i \\ & + \sum_{(i,j)\in\mathcal{E}} \mu_{ij} G_{ij} (V_i - V_j)^2 - \sum_{(i,j)\in\mathcal{E}} \mu_{ij} c_{ij}, \end{aligned}$$

where $\boldsymbol{\lambda}$ and $\boldsymbol{\mu}$ are the nonnegative dual variables associated with the constraints $\mathbf{V}^T\mathbf{G}_j\mathbf{V} \le \overline{p}_i \ \forall i \in \mathcal{N}$ and $\mathbf{V}^T\mathbf{G}_{ij}\mathbf{V} \le c_{ij} \ \ \forall (i,j) \in \mathcal{E}$ respectively. For any given feasible λ_i at each bus and μ_{ij} at each line, consider the following partial Lagrangian minimization problem:

$$\begin{array}{ll} \text{minimize} & L(\mathbf{V}, \{\boldsymbol{\lambda}, \boldsymbol{\mu}\}) \\ \text{subject to} & \underline{V}_i \le V_i \le \overline{V}_i \ \ \forall i \in \mathcal{N}. \end{array} \tag{7}$$

Note that (7) is nonconvex in $\mathbf{V}$. However, since the objective is smooth and by using the Slater's condition that guarantees the existence of the interior of a feasible constraint set, the optimal solution to (7) must satisfy the Karush-Kuhn Tucker (KKT) conditions. By rewriting the KKT conditions, it can be shown that the optimal solution must satisfy:

$$\mathbf{V} = \max\left\{\underline{\mathbf{V}}, \min\left\{\overline{\mathbf{V}}, \mathbf{B}(\boldsymbol{\lambda}, \boldsymbol{\mu})\mathbf{V}\right\}\right\}, \tag{8}$$

where the nonnegative matrix $\mathbf{B}$[3] has entries in terms of $\boldsymbol{\lambda}$ and $\boldsymbol{\mu}$:

$$B_{ij} = \begin{cases} \dfrac{2G_{ij} + \lambda_i G_{ij} + \lambda_j G_{ij} + 2\mu_{ij} G_{ij}}{2\left((1+\lambda_i) \sum\limits_{j\in\Omega_i} G_{ij} + \sum\limits_{(i',j')\in\mathcal{E}} \mu_{i'j'} G_{i'j'}\right)} & \forall (i,j) \in \mathcal{E} \\ 0 & \text{otherwise.} \end{cases} \tag{9}$$

Suppose that the optimal dual variables $\boldsymbol{\lambda}^*$ and $\boldsymbol{\mu}^*$ of (3) are given (recall that they exist due to the zero duality gap), then the optimal voltage $\mathbf{V}^*$ must satisfy $\mathbf{V}^* = \max\left\{\underline{\mathbf{V}}, \min\left\{\overline{\mathbf{V}}, \mathbf{B}(\boldsymbol{\lambda}^*, \boldsymbol{\mu}^*)\mathbf{V}^*\right\}\right\}$.

It is interesting to ask whether $\mathbf{V}^*$ is unique. There are several ramifications to the solvability of (3) by the convex relaxation (4) and also to solving (3) using distributed algorithms (also see Remark 3 later). To prove uniqueness, we leverage a result in [28], [29] to inspect the generalized critical points of $\nabla L(\mathbf{V}, \{\boldsymbol{\lambda}, \boldsymbol{\mu}\})$ (the first order derivative of $L(\mathbf{V}, \{\boldsymbol{\lambda}, \boldsymbol{\mu}\})$ with respect to $\mathbf{V}$) over the box constraint set in (7). We first state the definition of the P-matrix and the result in [28].

[3]The nonnegative matrix $\mathbf{B}$ is irreducible since the graph of the power network is fully connected, i.e., $\mathbf{G}$ is irreducible. By the Perron-Frobenius theorem (cf. Proposition 6.6 in [31]), its spectral radius $\rho(\mathbf{B})$ is an eigenvalue of $\mathbf{B}$ (the Perron-Frobenius eigenvalue). Also, $\rho(\mathbf{B})$ is simple and positive, and the right and left eigenvectors corresponding to $\rho(\mathbf{B})$ are positive.

Definition 1 ([28], Definition 1): An $n \times n$ matrix A is a P-matrix if all the determinants of its principal sub-matrices are positive, i.e. $\det(\mathbf{A}|J) > 0$, $\forall J \subset \{1, 2, \ldots, n\}$.

Lemma 2 ([28], Corollary 1): Let M be a box-constrained region. Let U be an open set containing M, and $f : U \to \mathbb{R}$ be a twice differentiable function. Let KKT (f, M) denote the Karush-Kuhn-Tucker stationary points of f over the region M and assume that for every $x \in \text{KKT}(f, M), H(x)|_{I^{\nabla f(x)}}$ is a P-matrix, where $H(x)|_{I^{\nabla f(x)}}$ denotes the principal submatrix of the Hessian matrix $H(x)$ containing precisely the entries H_{ij} where $i, j \in I^{\nabla f}(x)$ and $I^{\nabla f}(x) = \{i \in \{1, 2, \ldots, N\} | \nabla f_i = 0\}$. Then, KKT$(f, M)$ has a unique element which is also the unique local (global) minimum of f over M.

Now, the derivative of $\nabla L(\mathbf{V}, \{\boldsymbol{\lambda}, \boldsymbol{\mu}\})$, i.e., the Hessian in (7), is given by a square matrix in terms of $\{\boldsymbol{\lambda}, \boldsymbol{\mu}\}$. Let us denote this Hessian matrix by $\mathbf{A}$. Clearly, the uniqueness of the solution in (3) depends on the network topology (as $\mathbf{A}$ contains $\mathbf{G}$ and $\mathbf{G}_{ij}$) and the dual variables (how they pair up with the optimal primal variable $\mathbf{V}^*$ to satisfy the KKT conditions). In the following, we study the application of Lemma 2 to this Hessian matrix $\mathbf{A}$ using simple network topologies for illustration.

Example 1: We study the uniqueness of the solution in (3) for a 2-bus line network as shown in Figure 1(a) with a generator at bus 1 and a load at bus 2. Also, $\overline{p}_1 > 0$ and $\overline{p}_2 < 0$. Then the Hessian $\mathbf{A}$ in (7) is given by $\mathbf{A} = (\mathbf{G} + \lambda_1 \mathbf{G}_1 + \lambda_2 \mathbf{G}_2 + \mu_{12} \mathbf{G}_{12})$. We first use the spectral property of $\mathbf{B}$ in (9) to show that at least one of the box constraints is binding. Now, the Perron-Frobenius eigenvalue $\rho(\mathbf{B})$ and its right eigenvector of $\mathbf{B}$ are given respectively as:

$$\rho(\mathbf{B}) = \frac{\lambda_1 + \lambda_2 + 2 + 2\mu_{12}}{2\sqrt{(\mu_{12} + 1 + \lambda_1)(\mu_{12} + 1 + \lambda_2)}}$$

and

$$\begin{pmatrix} \frac{\lambda_1 + \lambda_2 + 2 + 2\mu_{12}}{2\sqrt{(\mu_{12}+1+\lambda_1)(\mu_{12}+1+\lambda_2)}} \\ \frac{\lambda_1 + \lambda_2 + 2 + 2\mu_{12}}{2(\mu_{12}+1+\lambda_2)} \end{pmatrix}.$$

Observe that $\rho(\mathbf{B}) \geq 1$ in the above. In fact, $\rho(\mathbf{B}) = 1$ if and only if $\lambda_1 = \lambda_2$ and the right eigenvector is proportional to the all-one vector. Hence, if $\mathbf{V}^* = \mathbf{B}\mathbf{V}^*$, then $V_1 = V_2$, i.e., no power flows to bus 2, which is infeasible. Thus, $\lambda_1 \neq \lambda_2$ at optimality and $\mathbf{V}^*$ is not in the interior of the box constraint, i.e., at least one of the box constraints is binding.

Next, it is easy to see that $\mathbf{A}$ is nonsingular and it can be shown that the determinant of the principal submatrix (a scalar) of $\mathbf{A}$ is given by $(1 + \lambda_i + \mu_{12})G_{12}$, $i = 1$ or 2, which is always positive. Using Lemma 2, (7) has a unique solution. To illustrate, Figure 1(b) plots the solution space over V_1 and V_2 in the box constraint $[1, 2]$ for fixed dual variables, and there is only one optimal solution, i.e., $V_1 = 2V$, $V_2 = 1.5V$.

Moreover, we have the following relationships:

$$\frac{V_1^*}{V_2^*} = \frac{2 + \lambda_1 + \lambda_2 + 2\mu_{12}}{2 + 2\lambda_1 + 2\mu_{12}}, \text{ if the box constraint of } V_2^* \text{ is binding,}$$

$$\frac{V_2^*}{V_1^*} = \frac{2 + \lambda_1 + \lambda_2 + 2\mu_{12}}{2 + 2\lambda_2 + 2\mu_{12}}, \text{ if the box constraint of } V_1^* \text{ is binding.}$$

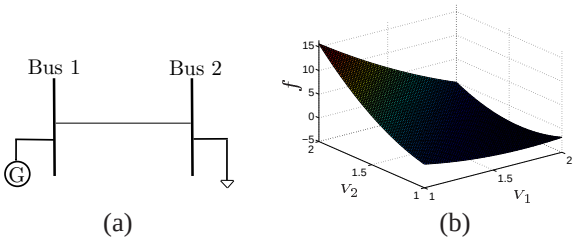

Fig. 1. (a) In this example, two connected buses (bus 1 and bus 2) are respectively attached by a generator and a load. (b) The value of f by varying V_1 and V_2 for fixed dual variables.

Note that λ_1 and λ_2 are inversely proportional to the nodal voltage, and furthermore $\lambda_2 > \lambda_1$. This has the natural interpretation that the price to be paid at bus 2 by the demand is strictly greater than the price to generate the power (since power is necessarily lost over transmission).

Example 2: We consider a general $(n+1)$-bus line network as shown in Figure 2(a). In this case, the Hessian matrix $\mathbf{A}$ is a symmetric tridiagonal matrix:

$$\mathbf{A} = \begin{pmatrix} A_{11} & -A_{12} & & & & \\ -A_{12} & A_{22} & -A_{23} & & & \\ & -A_{23} & \ddots & \ddots & & \\ & & \ddots & \ddots & -A_{n(n+1)} & \\ & & & -A_{n(n+1)} & A_{(n+1)(n+1)} \end{pmatrix},$$

where

$$A_{ij} = \begin{cases} (1 + \lambda_1 + \mu_{12})G_{12}, & i = j = 1 \\ (1 + \lambda_{n+1} + \mu_{n(n+1)})G_{n(n+1)}, & i = j = n+1 \\ (1 + \lambda_i + \mu_{(i-1)i})G_{(i-1)i} & i = j = 2, \ldots, n \\ +(1 + \lambda_i + \mu_{i(i+1)})G_{i(i+1)}, & \\ (\frac{\lambda_i}{2} + \frac{\lambda_j}{2} + \mu_{ij} + 1)G_{ij}, & j = i+1 \text{ or } i-1 \\ 0, & \text{Otherwise.} \end{cases}$$

Let us first consider the case when $n = 2$ to compute the Perron-Frobenius eigenvalue of $\mathbf{B}$. Solving the characteristic equation for the eigenvalues of $\mathbf{B}$: $x(x^2 - B_{23}B_{32} - B_{12}B_{21}) = 0$, it is easy to show that $\rho(\mathbf{B}) = \sqrt{B_{23}B_{32} + B_{12}B_{21}}$. In particular, let $m_{12} = 1 + \lambda_1 + \mu_{12}$, $m_{21} = 1 + \lambda_2 + \mu_{12}$, $m_{23} = 1 + \lambda_2 + \mu_{23}$ and $m_{32} = 1 + \lambda_3 + \mu_{23}$, then the Perron-Frobenius eigenvalue is:

$$\rho(\mathbf{B}) = \sqrt{\frac{(m_{12} + m_{21})^2 G_{12} m_{32} + (m_{23} + m_{32})^2 G_{23} m_{12}}{4m_{12}m_{21}m_{32}G_{12} + 4m_{12}m_{23}m_{32}G_{23}}}.$$

Since $m_{12} + m_{21} \geq 2\sqrt{m_{12}m_{21}}$ and $m_{23} + m_{32} \geq 2\sqrt{m_{23}m_{32}}$, we have $\rho(\mathbf{B}) \geq \sqrt{\frac{4m_{12}m_{21}m_{32}G_{12} + 4m_{12}m_{23}m_{32}G_{23}}{4m_{12}m_{21}m_{32}G_{12} + 4m_{12}m_{23}m_{32}G_{23}}} = 1$. Thus, at least one of the nodal voltage constraints is binding. For example, when V_1^* has a binding box constraint, we delete the first row and the first column of $\mathbf{A}$ and use Lemma 2 to check whether the following reduced 2×2 matrix $\mathbf{A}_{2\times 2}$ is a P-matrix:

$$\mathbf{A}_{2\times 2} = \begin{pmatrix} A_{22} & -A_{23} \\ -A_{23} & A_{33} \end{pmatrix}.$$

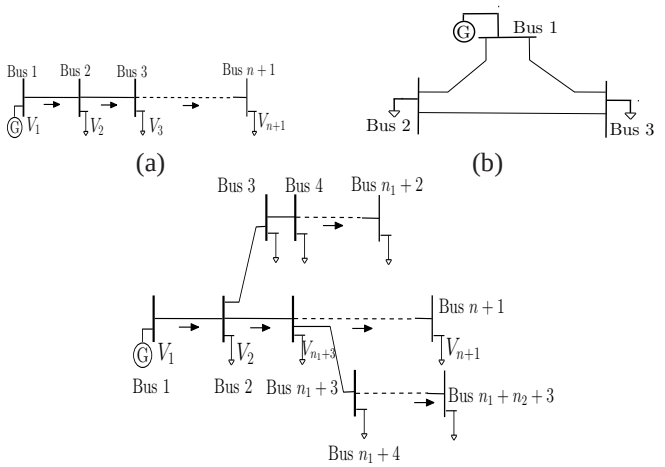

Fig. 2. Different power network topologies in which bus 1 is connected to a generator and the other buses are connected to loads. (a) A line network. The power generated at bus 1 is transmitted to satisfy these loads at the successive n buses. (b) A mesh network that consists of three buses where two have loads. (c) A radial network with a total of n buses and having two branches (n_1 and n_2 buses on the branches rooted at bus 2 and bus 3 respectively).

By elementary row operations, we have the following upper triangular matrix

$$\mathbf{A}'_{2\times 2} = \begin{pmatrix} A_{22} & -A_{23} \\ 0 & A_{33} - A_{23}^2/A_{22} \end{pmatrix}.$$

Next, from (7) and the relationship between $\mathbf{A}$ and $\mathbf{B}$, i.e., $B_{ij} = A_{ij}/A_{ii}$ if $(i,j) \in \mathcal{E}$ and $B_{ij} = 0$, otherwise, we have $A_{33} - A_{23}^2/A_{22} = A_{23}\frac{V_2^*}{V_3^*} + \frac{A_{12}A_{23}}{A_{22}}\frac{V_1^*}{V_3^*} - A_{23}\frac{V_2^*}{V_3^*} > 0$. Thus, the determinant of the upper triangular matrix $\mathbf{A}'_{2\times 2}$ is positive, which implies that all the principal minors of $\mathbf{A}_{2\times 2}$ are positive. Therefore, using Lemma 2, we conclude that the optimal solution is unique when V_1^* is binding.

On the other hand, if V_2^* has a binding box constraint, then the reduced matrix $\mathbf{A}_{2\times 2}$ becomes

$$\mathbf{A}_{2\times 2} = \begin{pmatrix} A_{11} & 0 \\ 0 & A_{33} \end{pmatrix},$$

which is a P-matrix, and thus the optimal solution is unique. Since bus 1 and bus 3 are symmetric in the line network, we can also deduce that the optimal solution is unique when V_3^* has a binding box constraint. Lastly, if the voltages of any two buses have binding box constraints, then the reduced matrix only contains one positive element, which implies that the optimal solution is unique. To summarize, the optimal solution in the 3-bus line network is unique.

Example 3: We consider a mesh network with three buses as shown in Figure 2(b). The Hessian matrix $\mathbf{A}$ is

$$\mathbf{A} = \begin{pmatrix} A_{11} & -A_{12} & -A_{13} \\ -A_{12} & A_{22} & -A_{23} \\ -A_{13} & -A_{23} & A_{33} \end{pmatrix},$$

where $A_{11} = (1+\lambda_1+\mu_{12})G_{12} + (1+\lambda_1+\mu_{13})G_{13}, A_{33} = (1+\lambda_3+\mu_{23})G_{23} + (1+\lambda_3+\mu_{13})G_{13}$, $A_{13} = (1+\lambda_1/2+\lambda_3/2+\mu_{13})G_{13}$ and all the other parameters being the same as that in the 3-bus line network.

Suppose that V_1^* has a binding box constraint, then the reduced matrix is the same as that in the 3-bus line network where V_1^* is binding. Checking the determinant of the submatrix, we have: $A_{33} - A_{23}^2/A_{22} = A_{13}\frac{V_1^*}{V_3^*} + A_{23}\frac{V_2^*}{V_3^*} + \frac{A_{12}A_{23}}{A_{22}}\frac{V_1^*}{V_3^*} - A_{23}\frac{V_2^*}{V_3^*} > 0$, which implies that the submatrix is a P-matrix. Thus, we conclude that the optimal solution is unique when V_1^* is binding. The same argument can also be applied to buses 2 and 3 to deduce that the optimal solution is unique when either V_2^* or V_3^* has a binding box constraint. Likewise, if the voltages of any two buses have binding box constraints, the optimal solution is unique.

The above three examples illustrate how to exploit the non-negativity (of the problem variables and parameters) inherent in the problem to prove uniqueness for simple network topologies. We now turn to two more general network topologies, namely the line network (for general n) and the radial network as shown in Figure 2(a) and Figure 2(c) respectively. We first state the following result.

Lemma 3: For a resistive radial network OPF, at least one of the buses has the binding voltage box constraint at optimality.

Proof: For a network that consists of n buses, assume that none of the buses has a tight box constraint and $\mathbf{V}^*$ is a feasible solution to (3). Then, we have $\mathbf{V}^* = \mathbf{B}\mathbf{V}^*$, i.e., $A_{ii} = \sum_{j\in\Omega_i}\frac{V_j^*}{V_i^*}A_{ij} \quad \forall i \in \mathcal{N}$. Moreover, we can deduce that the sum of all the elements in $\mathbf{A}$ equals zero, i.e., $\sum_{i\in\mathcal{N}} A_{ii} - \sum_{j\in\Omega_i} 2A_{ij} = 0$. Therefore, we have the condition that $\sum_{(i,j)\in\mathcal{E}}(2 - \frac{V_j^*}{V_i^*} - \frac{V_i^*}{V_j^*})A_{ij} = 0$. However, since $(V_i - V_j)^2 \geq 0$, this implies the condition $\frac{V_j^*}{V_i^*} + \frac{V_i^*}{V_j^*} \geq 2 \ \ \forall (i,j) \in \mathcal{E}$. Combining these two conditions, it implies that $V_1^* = V_2^* = \ldots = V_n^*$, i.e., $\mathbf{V}^*$ is proportional to the all-one vector and in this case $\mathbf{B}$ is a row stochastic matrix. However, this violates the nodal demand constraint, and hence $\mathbf{V}^*$ is infeasible thereby contradicting the assumption. This completes the proof. ■

Remark 2: Lemma 3 has the following physical interpretation: whenever the voltage is increased, the line losses are reduced. As such, the total costs can be reduced by uniformly increasing all the voltages until a voltage limit is reached.

For example, in the 3-bus mesh network, if none of the voltage constraints is binding, then we have: $A_{11} = \frac{V_2^*}{V_1^*}A_{12} + \frac{V_3^*}{V_1^*}A_{13}, A_{22} = \frac{V_1^*}{V_2^*}A_{12} + \frac{V_3^*}{V_2^*}A_{23}, A_{33} = \frac{V_1^*}{V_3^*}A_{13} + \frac{V_2^*}{V_3^*}A_{23}$. Then, by summing the left-hand side and the right-hand side of these three equations and leveraging the fact that $A_{11} + A_{22} + A_{33} - 2A_{12} - 2A_{13} - 2A_{23} = 0$, we have: $(2 - \frac{V_2^*}{V_1^*} - \frac{V_1^*}{V_2^*})A_{12} + (2 - \frac{V_3^*}{V_1^*} - \frac{V_1^*}{V_3^*})A_{13} + (2 - \frac{V_3^*}{V_2^*} - \frac{V_3^*}{V_2^*})A_{23} = 0$. Therefore, we have $V_1^* = V_2^* = V_3^*$, which is infeasible (no power flows from bus 1 to buses 2 and 3).

We now state the key result on the uniqueness of the optimal solution in (3).

Theorem 1: The optimal solution of (3) is unique in a resistive network with a radial network topology.

Remark 3: There are several implications on the uniqueness of $\mathbf{V}^*$. Note that (8) implies that the Lagrange dual function is smooth at the optimality of (3). The smoothness of the Lagrange dual at optimality implies that the optimal dual variables are unique and stable, and thus can be suitably used as power and line prices in pricing schemes. More importantly, it enlarges the space of designing simple local algorithms with low complexity to solve (3), and we address this in the following section.

V. Local Algorithms

In this section, we design simple local algorithms to solve (3). This is achieved by first solving (7) for given $\{\boldsymbol{\lambda}, \boldsymbol{\mu}\}$, and then using the projected gradient method in [30] to update the dual variables, which in turn are used as the input to solving (7) iteratively.

We propose the following fixed point algorithm that computes the fixed point $\mathbf{V}$ in (8) for a given set of feasible dual variables $\boldsymbol{\lambda}$ and $\boldsymbol{\mu}$.

Algorithm 1:

Compute voltage $\mathbf{V}$:

$$V_i(k+1) = \max\left\{\underline{V}_i, \min\left\{\overline{V}_i, \sum_{j\in\Omega_i} B_{ij}V_j(k)\right\}\right\}, \quad (10)$$

for all $i \in \mathcal{N}$, where B_{ij} is given in (9) for all i, j.

Theorem 2: Suppose (7) has a unique optimal solution. Then, given any $\mathbf{V}(0)$ which satisfies $\underline{\mathbf{V}} \le \mathbf{V}(0) \le \overline{\mathbf{V}}$, $\mathbf{V}(k)$ in Algorithm 1 converges to the unique optimal solution of (7).

Proof: Let $\mathbf{f}(\mathbf{V}) = \max\{\underline{\mathbf{V}}, \min\{\overline{\mathbf{V}}, \mathbf{B}\mathbf{V}\}\}$. First, we show that if $\mathbf{V}(0) = \underline{\mathbf{V}}$, then $\mathbf{V}(k)$ is a monotonic increasing and bounded sequence. Clearly, we have $\mathbf{V}(1) \ge \mathbf{f}(\mathbf{V}(0)) \ge \underline{\mathbf{V}} = \mathbf{V}(0)$. Now, observe that for any $\mathbf{V}(k)$ and $\mathbf{V}(k+1)$ satisfying $\mathbf{V}(k+1) \ge \mathbf{V}(k)$, we have

$$\mathbf{V}(k+2) = \mathbf{f}(\mathbf{V}(k+1)) \ge \mathbf{f}(\mathbf{V}(k)) = \mathbf{V}(k+1). \quad (11)$$

Here, the inequality follows from the fact that the entries of $\mathbf{B}$ are nonnegative. By induction, it follows that $\mathbf{V}(k)$ is a monotonic increasing sequence. Clearly, $\mathbf{V}(k) = \mathbf{f}(\mathbf{V}(k-1)) \le \overline{\mathbf{V}}$ for all k so it is bounded.

By a similar argument, we have that if $\mathbf{V}(0) = \overline{\mathbf{V}}$, then $\mathbf{V}(k)$ is a monotonic decreasing and bounded sequence.

Now, given any $\mathbf{V}(0)$ which satisfies $\underline{\mathbf{V}} \le \mathbf{V}(0) \le \overline{\mathbf{V}}$, we have

$$\lim_{k\to\infty} \mathbf{f}^k(\underline{\mathbf{V}}) \le \lim_{k\to\infty} \mathbf{f}^k(\mathbf{V}(0)) \le \lim_{k\to\infty} \mathbf{f}^k(\overline{\mathbf{V}}). \quad (12)$$

Since $\mathbf{f}^k(\underline{\mathbf{V}})$ is a monotonic increasing and bounded sequence, it must converge. By Theorem 1 there is a unique solution to $\mathbf{V} = \mathbf{f}(\mathbf{V})$. Hence $\mathbf{f}^k(\underline{\mathbf{V}})$ must converge to the unique fixed point. Let us denote by $\mathbf{V}^*$ the unique fixed point. Using a similar argument, we conclude that $\mathbf{f}^k(\overline{\mathbf{V}})$ must also converge to $\mathbf{V}^*$. Hence, we have $\mathbf{V}^* \le \lim_{k\to\infty} \mathbf{f}^k(\mathbf{V}(0)) \le \mathbf{V}^*$, which implies that $\lim_{k\to\infty} \mathbf{f}^k(\mathbf{V}(0)) = \mathbf{V}^*$. ■

Due to practical considerations on information exchange and computation time at each bus, some of the buses may execute less iterations or use outdated and asynchronous iterates for update. In the following, we study the asynchronous version of Algorithm 1.

Assumption 1: (Total asynchronism, [31], pp.430) Denote $\tau_j^i(k)$ as the most recent time for V_j that is known to bus i, where $0 < \tau_j^i(k) < k$, and K^i as the set of times where $V_i(k)$ is updated, i.e., $V_i(k)$ is unchanged at times $k \notin V_i(k)$. Assume the sets K^i are infinite. If k_t is a sequence of elements of K^i that tends to infinity, then $\lim_{t\to\infty} \tau_j^i(k_t) = \infty$ for every j.

Using Assumption 1, the convergence of the asynchronous version of Algorithm 1 is determined in the following:

Corollary 1: Suppose (7) has a unique optimal solution. Then, from any initial $\mathbf{V}(0)$ which satisfies $\underline{\mathbf{V}} \le \mathbf{V}(0) \le \overline{\mathbf{V}}$, $\mathbf{V}(k)$ in the totally asynchronous version of Algorithm 1 converges to the unique optimal solution of (7).

We next leverage Algorithm 1 together with a gradient projection method in [30] that updates the dual variables $\boldsymbol{\lambda}$ and $\boldsymbol{\mu}$ to solve (7) in the following.

Algorithm 2:

1) Set the stepsizes $\beta, \rho \in (0, 1)$.
2) Run Algorithm 1 with input $\lambda_i(t)$ and $\mu_{ij}(t)$ for the entries of $\mathbf{B}$.
3) Compute:

$$\lambda_i(t+1) = \max\{0, \lambda_i(t) + \beta(\sum_{j\in\Omega_i} G_{ij}V_i(k)(V_i(k) - V_j(k)) - \overline{p}_i)\}, \quad (13)$$

for all $i \in \mathcal{N}$.

$$\mu_{ij}(t+1) = \max\{0, \mu_{ij}(t) + \rho(G_{ij}(V_i(k) - V_j(k))^2 - c_{ij})\}, \quad (14)$$

for all $(i, j) \in \mathcal{E}$.

Update the stepsizes β and ρ according to Theorem 3.

Theorem 3: Assume that $V_i(k)$ and $\hat{V}_i(k)$ denote the (prematurely terminated) approximated and the exact solution (on convergence) at step 2 of Algorithm 2 for $\lambda_i(t)$ and $\mu_{ij}(t)$, respectively. Suppose the output of Algorithm 1 satisfies

$$\sum_{i\in\mathcal{N}} \limsup_k |\sum_{j\in\Omega_i} G_{ij}\hat{V}_i(k)(\hat{V}_i(k) - \hat{V}_j(k)) - \overline{p}_i| \le \epsilon_1$$

and

$$\sum_{(i,j)\in\mathcal{E}} \limsup_k |G_{ij}(\hat{V}_j(k) - \hat{V}_i(k))^2 - c_{ij}| \le \epsilon_2$$

for some sufficiently small positive ϵ_1 and ϵ_2. We choose the diminishing stepsizes $\beta(t)$ and $\rho(t)$ to satisfy

$$\sum_{t=0}^{\infty} \beta(t) = \infty, \ \sum_{t=0}^{\infty} (\beta(t))^2 < \infty, \sum_{t=0}^{\infty} \rho(t) = \infty, \ \sum_{t=0}^{\infty} (\rho(t))^2 < \infty.$$

Then $\boldsymbol{\lambda}(t+1)$ and $\boldsymbol{\mu}(t+1)$ converge to a closed neighborhood of $\boldsymbol{\lambda}^*$ and $\boldsymbol{\mu}^*$ when $t \to \infty$, respectively.

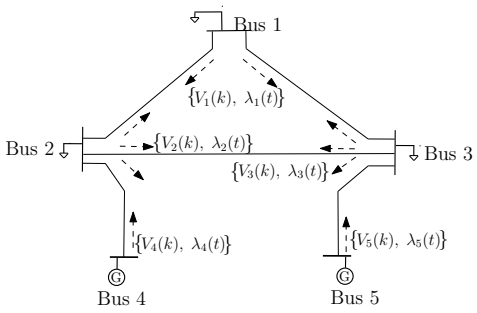

Fig. 3. Message passing in a 5-bus system ([32], Chapter 6, pp.327).

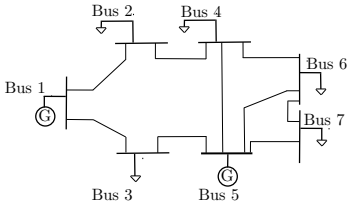

Fig. 4. An example with 7 buses and 9 lines.

Remark 4: Note that computing (10) is approximately optimal due to the finite iterations in the inner loop. These errors can accumulate and lead to an approximated (instead of the exact) gradient computed in (13). The proof of Theorem 3 is based on the approximated gradient projection method in [30]. Theorem 3 shows that the (sufficiently small) errors do not affect the asymptotic convergence so long as the stepsizes are chosen appropriately. In Section VI, we illustrate that the optimal solution obtained by Algorithm 2 is arbitrarily close to the solution obtained by centralized interior point methods.

A. Further Discussions

Algorithm 2 can be run in a distributed manner using message passing to transmit and receive iterates of the voltage and dual variables with neighboring one-hop buses. This is illustrated in Figure 3 for a 5-bus system ([32], Ch.6, pp.327). Each bus $i \in \mathcal{N}$ randomly chooses a feasible $V_i(0)$ and broadcast to its neighbors. Once a bus $i \in \mathcal{N}$ receives all V_j where $j \in \Omega_i$, it calculates λ_i and μ_{ij} according to (13) and (14). Next, the updated λ_i is sent to its neighbors. Since μ_{ij} can be obtained at each pair of neighboring buses, there is no need to exchange μ_{ij}. After collecting all λ_j $(j \in \Omega_i)$, V_i can be calculated by (10) at bus i. This is repeated until convergence.

The dual variables $\{\boldsymbol{\lambda}, \boldsymbol{\mu}\}$ have a shadow price interpretation (cf. Chapter 5 in [16]) in the sense that $\boldsymbol{\lambda}^*$ and $\boldsymbol{\mu}^*$ are the equilibrium prices for the resource availability of the nodal power and line capacity respectively. For example, at bus i, we increase the price λ_i if $\mathbf{V}^T\mathbf{G}_i\mathbf{V} - \overline{p}_i \geq 0$ and decrease it otherwise. As future work, it is interesting to understand how Algorithms 1 and 2 can be used in Locational Marginal Pricing (LMP) scheme.

VI. Numerical Examples

In this section, we first compare the computational efficiency of our SOCP relaxation approach with the state-of-the-art SDP relaxation approach in [17], [19]. Then, we evaluate the performance of our proposed local algorithms.

A. Efficiency of SOCP relaxation vs SDP relaxation

We compare the running time of our SOCP relaxation and the SDP relaxation in [17], [19] by using the SEDUMI solver that is integrated into the CVX optimization package [27] to solve (3) on a desktop computer with an Intel-i7 CPU and 4G RAM. We consider various IEEE system (a 14-bus system, a 57-bus system, a 118-bus system and a 300-bus system) extracted from [33]. We also use a 500-bus system with 561 lines from a 1999-2000 winter Polish system data that is available in the MATPOWER toolbox [34]. We obtain the resistive networks from the AC networks by discarding the reactance values, and, for line parameters whose resistance values are not specified, we choose the resistance pu (per unit)[4] values randomly such that the OPF problem is feasible. We solve a hundred instances of the problem and record the average computation time in Table I, which shows that the SOCP relaxation is computationally more efficient than the SDP relaxation especially when the system scales up.

TABLE I
Average running time in seconds comparing the SOCP and the SDP relaxation.

Systems	SOCP	SDP [17], [19]
14-bus	0.070	0.074
57-bus	0.186	0.385
118-bus	0.297	1.982
300-bus	0.558	20.650
500-bus	0.667	1932.613

B. Evaluation of local algorithms

We evaluate the performance of Algorithm 2 using the example with 7 buses and 9 lines and a 5-bus system example. For the 7-bus system, as shown in Figure 4, there are two generators, i.e., bus 1 and bus 5, and five demand buses with loads. For the 5-bus system (See Figure 3), bus 4 and bus 5 are the generators. The parameter settings are as follows. In the 7-bus system, the conductance for each line is $\mathbf{g} = [G_{12}\ \ G_{13}\ \ G_{24}\ \ G_{35}\ \ G_{45}\ \ G_{46}\ \ G_{56}\ \ G_{57}\ \ G_{67}]^T = [5\ \ 2\ \ 5\ \ 6\ \ 4\ \ 6\ \ 4\ \ 3\ \ 6]^T$pu. The power constraint $\overline{\mathbf{p}}$ is $[2.7306\ \ -0.6466\ \ -0.7046\ \ -0.6151\ \ 3.2626\ \ -0.5831\ \ -0.6571]^T$pu. In the 5-bus system, the conductance for each line is $\mathbf{g} = [G_{12}\ \ G_{13}\ \ G_{23}\ \ G_{24}\ \ G_{35}]^T = [4\ 3\ 4\ 6\ 7]^T$pu. The power constraint $\overline{\mathbf{p}}$ is $[-0.2468\ \ -\ 3.0204\ \ -$

[4]We thank an anonymous reviewer for suggesting the use of per unitization in order to achieve scale independence. The numerical examples given in a per unit system can be translated to the actual quantities in the real system by appropriately choosing a base power for the problem (typically 100 MVA for a bulk power system or 100 KVA for a microgrid) and assume that line conductances are given in Siemens.

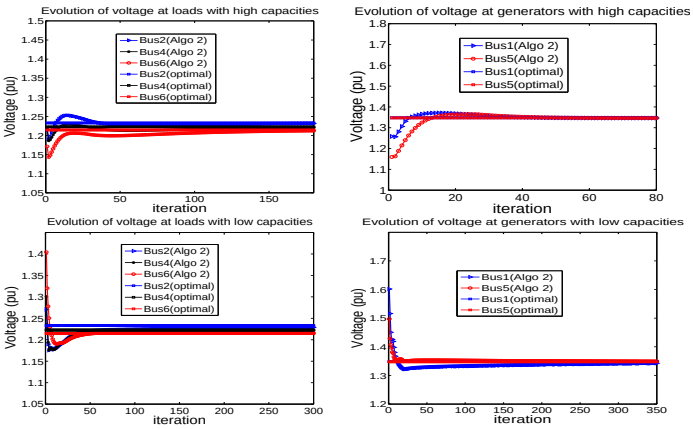

Fig. 5. Illustration of the convergence of Algorithm 2 in 7-bus system. The top two figures show the voltage convergence at loads (buses 2, 4 and 6) and generators in the high capacity lines scenario by choosing $\beta = 0.01$, respectively. The bottom two figures show the voltage convergence at loads (buses 2, 4 and 6) and generators in the low capacity lines scenario by choosing $\beta = 0.05, \rho = 0.2$, respectively.

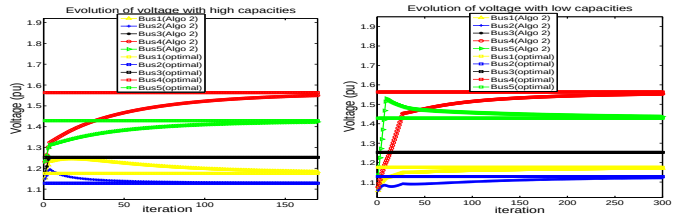

Fig. 6. Illustration of the convergence of Algorithm 2 in 5-bus system. The figures on the lefthand and the righthand side show the voltage convergence in the high capacity lines and the low capacity lines scenario respectively.

$0.32 \;\; 4.0203 \;\; 7.7234]^T$pu. For comparison, a baseline solution can be obtained numerically by the SOCP relaxation in using CVX. Numerically, we check that our examples satisfy the P-matrix requirement in Lemma 2, which implies that the optimal solution are unique.

1) Evaluation of algorithms under different capacity constraints: We first consider the high capacity case. We let each transmission line have a large enough capacity, e.g., we set the line capacity of each line as 3pu in the 7-bus system and 1pu in the 5-bus system, which leads to that none of the capacity constraint in (3) is tight. Thus, at optimality, $\mu_{ij}, \forall (i,j) \in \mathcal{E}$ are all zeros and only $\lambda_i, \forall i \in \mathcal{N}$ matter. We plot the iterations of Algorithm 2 for the 7-bus system at the top lefthand and righthand sides of Figure 5 for the loads and generators, respectively. The iterations for the 5-bus system are plotted on the lefthand side of Figure 6.

Next, we set the line capacities as $\mathbf{c} = [0.0664 \; 1.0097 \; 1.0008 \; 1.0284 \; 2.0624 \; 2.0004 \; 1.0707 \; 0.0671 \; 2.0017]^T$pu and $\mathbf{c} = [0.1021 \; 0.1313 \; 0.1938 \; 0.8432 \; 0.3459]^T$pu in the 7-bus and 5-bus systems respectively. We plot the iterations of Algorithm 2 at the bottom lefthand and righthand sides of Figure 5 for the loads and generators, respectively. We plot the iterations of Algorithm 2 for the 5-bus system on the righthand side of Figure 6. From Figures 5 and 6, we observe that Algorithm 2 have fast convergence time. In the high line capacity scenario, as only $\lambda_i, \forall i \in \mathcal{N}$ need to

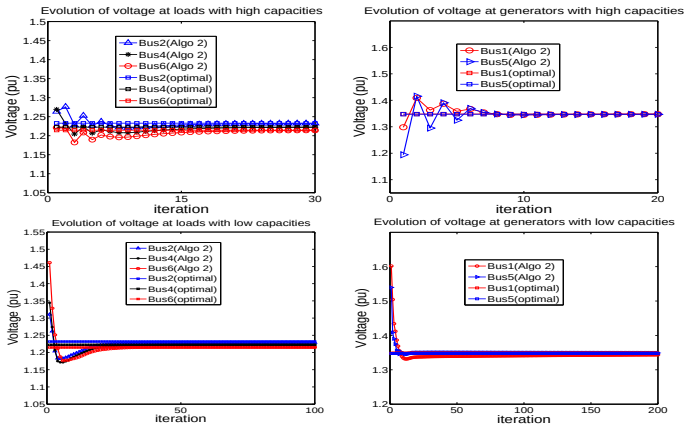

Fig. 7. Illustration of the convergence of Algorithm 2 in 7-bus system with a larger stepsize. The top two figures show the voltage convergence at loads (buses 2, 4 and 6) and generators in the high capacity lines scenario by choosing $\beta = 0.1$, respectively. The bottom two figures show the voltage convergence at loads (buses 2, 4 and 6) and generators in the low capacity lines scenario by choosing $\beta = 0.1, \rho = 0.2$, respectively.

be updated, convergence can be faster than the low capacity scenario (faster by 160 times in the 7-bus system and 150 times in the 5-bus system).

2) Evaluation of algorithms under different stepsizes: In this section, we study the effect of the stepsize on the algorithm convergence. Specifically, we repeat the above simulation in the 7-bus system with larger stepsizes, i.e. $\beta = 0.1$ in the high capacity case and $\beta = 0.1, \rho = 0.2$ in the low capacity line scenarios. When comparing the result in Figure 5 and Figure 7 we see that, by appropriately choosing a larger stepsize, our algorithms converge faster in both capacity cases.

3) Evaluation of algorithms in medium-sized IEEE systems: In this section, we evaluate the convergence performance of our proposed algorithms in medium-sized IEEE systems with more complex topologies. We use the IEEE 14-bus and 118-bus test systems for our simulation. The parameter setting of these two IEEE systems are the same as in Section VI-A. Moreover, we choose the line capacities at some of the lines to be low such that the dual variables can be positive, i.e., $\boldsymbol{\mu} \geq 0$. The initial values are randomly chosen to be feasible. In Figure 8, we plot the convergence performance at the generation buses and demand buses (buses 3, 6 and 12 in the figure) for the IEEE 14-bus system as well as the generation buses (buses 10 and 89 in the figure) and demand buses (buses 65, 66 and 86 in the figure) for the IEEE 118-bus system. We observe that a conservatively small stepsize has to be used for a larger system with more number of buses in order to ensure convergence stability, and convergence time typically scales linearly with the number of buses in the system.

VII. Conclusions

We studied a resistive network OPF problem for generation cost or transmission loss minimization, and proposed a SOCP relaxation under a load over-satisfaction assumption that is tight for this class of nonconvex quadratic constrained

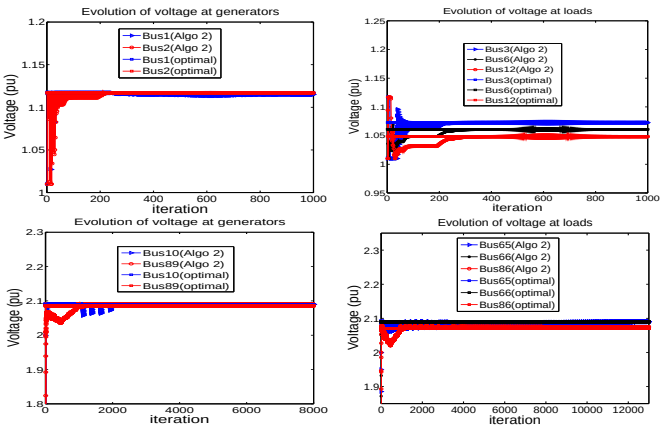

Fig. 8. Illustration of the convergence of Algorithm 2 in IEEE 14-bus system and IEEE 118-bus system with low capacity lines. The top two figures show the voltage convergence of the generators as well as demand buses 3, 6 and 12 in the IEEE 14-bus system. The bottom two figures show the voltage convergence of the generators buses 10 and 89 as well as demand buses 65, 66 and 86 in the IEEE 118-bus system.

quadratic programming problems. Leveraging a recently-discovered result of the zero duality gap in the OPF, we characterized the uniqueness of its solution using differential topology especially the Poincare–Hopf Index Theorem, and characterized its global uniqueness for a number of network topologies, e.g., a mesh network, general line-network and radial network. Based on the uniqueness characterization, we proposed distributed local algorithms with low complexity that synchronously or asynchronously converged to the unique global optimal solution of the resistive network OPF. Numerical evaluations showed that the SOCP relaxation is computationally more efficient than the SDP counterparts.

As future work, it is interesting to generalize our analysis and algorithm design methodologies to more general OPF problem formulations, e.g., an OPF problem that considers reactive components and has line flow constraints (which can be reformulated as a conic program) and more general network topologies. Another promising direction for future research is to examine the implications of the local algorithms and to shed further insights between the physics of power flow and economic dispatch pricing, e.g., LMP pricing.

VIII. Acknowledgement

The authors acknowledge helpful discussions with Steven Low at the California Institute of Technology.

IX. Appendix

A. Proof of Theorem 1

Let us first consider the $(n+1)$-bus line network. The idea is to extend the argument for the special case of $n=2$ to the general case by first transforming the matrix $\mathbf{A}$ to an upper triangular matrix, and then using (7) and the relationship between $\mathbf{A}$ and $\mathbf{B}$ to deduce uniqueness. Without loss of generality, assume that bus $i-1$ has a binding constraint, then $A_{(i-1)i}$ and $A_{i(i-1)}$ have been deleted. We proceed to check whether the upper triangular form $\mathbf{A}'$ of $\mathbf{A}$ after deleting both the $(i-1)$th row and column is a P-matrix. Due to the symmetry in $\mathbf{A}$ between the submatrices $\mathbf{A}_{(i-2)\times(i-2)}$ (the upper matrix after deletion) and $\mathbf{A}_{(n-i+2)\times(n-i+2)}$ (the lower matrix after deletion), we only focus on the submatrix $\mathbf{A}_{(n-i+2)\times(n-i+2)}$ in the following. By using the relationship between $\mathbf{A}$ and $\mathbf{B}$, we obtain the ith diagonal element of the upper triangular matrix as: $A'_{ii} = \frac{-A^2_{i(i+1)}}{A_{ii}} + A_{(i+1)(i+1)} = \frac{A_{(i-1)i}A_{i(i+1)}}{A_{ii}}\frac{V^*_{i-1}}{V^*_{i+1}} + A_{(i+1)(i+2)}\frac{V^*_{i+2}}{V^*_{i+1}} > 0$. For the next row, we have: $A'_{(i+1)(i+1)} = \frac{-A^2_{(i+1)(i+2)}}{A'_{ii}} + A_{(i+2)(i+2)} = \frac{-A^2_{(i+1)(i+2)}}{A'_{ii}} + A_{(i+1)(i+2)}\frac{V^*_{i+1}}{V^*_{i+2}} + A_{(i+2)(i+3)}\frac{V^*_{i+3}}{V^*_{i+2}}$. If we let $w_i = \frac{A_{(i-1)i}A_{i(i+1)}}{A_{ii}}\frac{V^*_{i-1}}{V^*_{i+1}}$, we have:

$$\frac{A^2_{(i+1)(i+2)}}{w_i + A_{(i+1)(i+2)}\frac{V^*_{i+2}}{V^*_{i+1}}} < \frac{A^2_{(i+1)(i+2)}}{A_{(i+1)(i+2)}\frac{V^*_{i+2}}{V^*_{i+1}}} = A_{(i+1)(i+2)}\frac{V^*_{i+1}}{V^*_{i+2}}.$$

Let $w_{i+1} = A_{(i+1)(i+2)}\frac{V^*_{i+1}}{V^*_{i+2}} - \frac{A^2_{(i+1)(i+2)}}{w_i + A_{(i+1)(i+2)}\frac{V^*_{i+2}}{V^*_{i+1}}}$. Then, we have: $A'_{(i+1)(i+1)} = w_{i+1} + A_{(i+2)(i+3)}\frac{V^*_{i+3}}{V^*_{i+2}} > 0$. By repeating this process to the remaining rows, we can deduce that the diagonal element of the upper triangular matrix is positive. In addition, for any subset of the buses that has the binding voltage constraints, the above process can be used to yield positive diagonal elements. Thus, we conclude that the submatrix is a P-matrix and, by using Lemma 2, the optimal solution of OPF in the line-network is unique.

Next, let us consider the radial network as shown in Figure 2(c). We first consider a special case in which each bus i has at most one branch bus attached, and we call this the *radial-s* topology. Let us further consider only the first four buses. Then, the submatrix $\mathbf{A}_{4\times4}$ is given by:

$$\mathbf{A}_{4\times4} = \begin{pmatrix} A_{11} & -A_{12} & 0 & 0 \\ -A_{12} & A_{22} & -A_{23} & -A_{24} \\ 0 & -A_{23} & A_{33} & 0 \\ 0 & -A_{24} & 0 & A_{44} \end{pmatrix}.$$

Similarly to the proof for the line-network, we first transform $\mathbf{A}_{4\times4}$ into an upper triangular matrix by performing the elementary operation to the fourth row and then use the fact that $V_3^*A_{33} = V_2^*A_{23}$ and $V_4^*A_{44} = V_2^*A_{24}$ to obtain:

$$\mathbf{A}'_{4\times4} = \begin{pmatrix} A_{11} & -A_{12} & 0 & 0 \\ -A_{12} & A_{22} & -A_{23} & -A_{24} \\ 0 & -A_{23} & A_{33} & 0 \\ 0 & 0 & -\frac{V_4^*}{V_3^*}A_{44} & A_{44} \end{pmatrix}.$$

By performing the elementary operation to the first two rows, we have:

$$\mathbf{A}''_{4\times4} = \begin{pmatrix} A_{11} & -A_{12} & 0 & 0 \\ 0 & A'_{22} & -A_{23} & -A_{24} \\ 0 & -A_{23} & A_{33} & 0 \\ 0 & 0 & -\frac{V_4^*}{V_3^*}A_{44} & A_{44} \end{pmatrix},$$

where $A'_{22} = A_{22} - \frac{A^2_{12}}{A_{11}} = \frac{V_1^*A_{12}+V_3^*A_{23}+V_4^*A_{24}}{V_2^*} - \frac{V_1^*A_{12}}{V_2^*} = \frac{V_3^*A_{23}+V_4^*A_{24}}{V_2^*} > 0$. Next, by repeating the elementary opera-

tion to the remaining rows, we have:

$$\mathbf{A}'''_{4\times 4} = \begin{pmatrix} A_{11} & -A_{12} & 0 & 0 \\ 0 & A'_{22} & -A_{23} & -A_{24} \\ 0 & 0 & A'_{33} & -\frac{A_{23}A_{24}}{A'_{22}} \\ 0 & 0 & 0 & A'_{44} \end{pmatrix},$$

where $A'_{33} = A_{33} - \frac{A_{23}^2}{A'_{22}} = A_{23}(\frac{V_2^*}{V_3^*} - \frac{A_{23}}{A'_{22}}) = A_{23}(\frac{V_2^*}{V_3^*} - \frac{A_{23}V_2^*}{A_{23}V_3^* + A_{24}V_4^*}) > 0$, and $A'_{44} = A_{44} - \frac{A_{23}A_{24}A_{44}V_4^*}{A'_{22}A'_{33}V_3^*} = A_{44} - \frac{A_{24}^2V_2^*}{V_4^*A_{24}} = A_{44} - \frac{A_{24}V_2^*}{V_4^*}$. If bus 4 is not the leaf bus in the radial topology, then $A_{44} > \frac{A_{24}V_2^*}{V_4^*}$, which implies that $A'_{44} > 0$. On the other hand, if bus 4 is a leaf bus, then $A'_{44} = 0$. If at least one of the buses has a binding voltage constraint, then we remove the corresponding row and column from $\mathbf{A}_{4\times 4}$, and use the above technique to deduce that every diagonal element in the resultant upper triangular matrix is positive.

Back to the radial-s case for a general number of buses (more than four), we can extend the above four-bus argument to the general case by induction. In particular, observe that, since each of the successive buses either has at most one branch bus or none, the matrix $\mathbf{A}$ is structurally identical to the above first-four buses case, i.e,

$$\mathbf{A} = \begin{pmatrix} A_{11} & -A_{12} & 0 & 0 & 0 & \cdots \\ -A_{12} & A_{22} & -A_{23} & -A_{24} & 0 & \cdots \\ 0 & -A_{23} & A_{33} & 0 & 0 & \cdots \\ 0 & -A_{24} & 0 & A_{44} & -A_{45} & \cdots \\ 0 & 0 & 0 & -A_{45} & A_{55} & \cdots \\ 0 & 0 & 0 & 0 & 0 & \cdots \\ \vdots & \vdots & \vdots & \vdots & \vdots & \cdots \end{pmatrix}.$$

Whenever bus i is not the branch bus, the elementary operation from bus i to bus $i+4$ (or less than 4 if no branch bus exists) does not affect the operation of other successive buses. By induction, we can deduce that the reduced submatrix of the radial-s (deleting the corresponding rows and columns from $\mathbf{A}$ accordingly) is a P-matrix.

Now, we can put together the above analysis for the radial-s and the line network to tackle the general radial network (whence bus i can have more than a single branch). In this general case, the $\mathbf{A}$ has a structure given as follows:

$$\mathbf{A} = \begin{pmatrix} A_{11} & -A_{12} & 0 & 0 & \cdots & 0 & \cdots \\ -A_{12} & A_{22} & -A_{23} & 0 & \cdots & -A_{2(n_1+3)} & \cdots \\ 0 & -A_{23} & A_{33} & -A_{34} & \cdots & 0 & \cdots \\ \vdots & \vdots & \ddots & \ddots & \ddots & 0 & \cdots \\ \vdots & -A_{2(n_1+3)} & \vdots & \ddots & \ddots & A_{(n_1+3)(n_1+3)} & \cdots \\ \vdots & \vdots & \vdots & \vdots & \vdots & \vdots & \ddots \end{pmatrix}.$$

Observe that, for each branch part, the elementary operation used in the line-network can be applied and that these operations do not affect the successive buses (for example, buses after bus n_1+3 in the above topology of $\mathbf{A}$). Suppose we have transformed the submatrix corresponding to the first n_1+2 buses to the upper triangular matrix (all the diagonal elements being positive according to the proof in the line network), then we have:

$$\mathbf{A}' = \begin{pmatrix} A_{11} & -A_{12} & 0 & 0 & \cdots & 0 & \cdots \\ 0 & A'_{22} & -A_{23} & 0 & \cdots & -A_{2(n_1+3)} & \cdots \\ 0 & 0 & A'_{33} & -A_{34} & \cdots & 0 & \cdots \\ \vdots & \vdots & \ddots & \ddots & \ddots & 0 & \cdots \\ \vdots & -A_{2(n_1+3)} & \vdots & \ddots & \ddots & A_{(n_1+3)(n_1+3)} & \cdots \\ \vdots & \vdots & \vdots & \vdots & \vdots & \vdots & \ddots \end{pmatrix}.$$

If we multiply the second row by $A_{2(n_1+3)}/A'_{22}$ and add it to the (n_1+3)th row, we have:

$$\mathbf{A}'' = \begin{pmatrix} A_{11} & -A_{12} & 0 & 0 & \cdots & 0 & \cdots \\ 0 & A'_{22} & -A_{23} & 0 & \cdots & -A_{2(n_1+3)} & \cdots \\ 0 & 0 & A'_{33} & -A_{34} & \cdots & 0 & \cdots \\ \vdots & \vdots & \ddots & \ddots & \ddots & 0 & \cdots \\ \vdots & 0 & A_{(n_1+3)3} & \ddots & \ddots & A'_{(n_1+3)(n_1+3)} & \cdots \\ \vdots & \vdots & \vdots & \vdots & \vdots & \vdots & \ddots \end{pmatrix},$$

where $A_{(n_1+3)3} = -A_{23}/A_{2(n_1+3)}$ and $A'_{(n_1+3)(n_1+3)} = A_{(n_1+3)(n_1+3)} - A^2_{2(n_1+3)}/A'_{22} = \frac{V_2^*A^2_{2(n_1+3)}}{V_3^*A_{23}} + \frac{V_{n_1+4}}{V_{n_1+3}}A_{(n_1+3)(n_1+4)} + \ldots > 0$. By repeating the above process from the third row to the (n_1+2)th row, i.e. multiplying the ith row by $A_{(n_1+3)i}/A'_{ii}$ and adding it to the (n_1+3)th row, where $i = 3, \ldots n_1+2$, we have:

$$\mathbf{A}''' = \begin{pmatrix} A_{11} & -A_{12} & 0 & 0 & \cdots & 0 & \cdots \\ 0 & A'_{22} & -A_{23} & 0 & \cdots & -A_{2(n_1+3)} & \cdots \\ 0 & 0 & A'_{33} & -A_{34} & \cdots & 0 & \cdots \\ \vdots & \vdots & \ddots & \ddots & \ddots & 0 & \cdots \\ \vdots & 0 & 0 & \ddots & \ddots & A'_{(n_1+3)(n_1+3)} & \cdots \\ \vdots & \vdots & \vdots & \vdots & \vdots & \vdots & \ddots \end{pmatrix}.$$

Now, we see that the submatrix corresponding to the second branch (the submatrix starting from $A'_{(n_1+3)(n_1+3)}$ to $A'_{(n_1+n_2+3)(n_1+n_2+3)}$) has a similar form as the submatrix starting from A'_{22} to $A'_{(n_1+2)(n_1+2)}$. Thus, by these elementary operations, we can transform all the following submatrices into diagonal submatrices. Moreover, from the analysis in the radial-s and the line-network, these submatrices have positive diagonals as long as there is at least one binding voltage constraint at one of the buses. Therefore, for the radial network, the reduced matrix is a P-matrix. If the branch part contains sub-branches, we can iteratively apply the above analysis to each of these sub-branches to deduce that the reduced submatrix is a P-matrix. Hence, by Lemma 2, the optimal solution of (3) in the radial network case is unique.

REFERENCES

[1] J. Carpentier. Contribution to the economic dispatch problem. *Bulletin de la Societe Francoise des Electriciens*, 3(8):431–447, 1962. In French.

[2] M. Huneault and F. D. Galiana. A survey of the optimal power flow literature. *IEEE Trans. on Power Systems*, 6(2):762–770, 1991.

[3] A. R. Bergen and V. Vittal. *Power Systems Analysis*. Prentice-Hall, Englewood Cliffs, NJ, 2nd edition, 2000.

[4] R. D. Christie, B. F. Wollenberg, and I. Wangensteen. Transmission management in the deregulated environment. *Proc. of IEEE*, 88(2):170–195, 2000.

[5] H. Wei, H. Sasaki, J. Kubokawa, and J. Yokoyama. An interior point nonlinear programming for optimal power flow problems with a novel data structure. *IEEE Trans. on Power Systems*, 13(3):870–877, 1998.

[6] A. J. Conejo and J. A. Aguado. Multi-area coordinated decentralized DC optimal power flow. *IEEE Trans. on Power Systems*, 13(4):1272–1278, 1998.

[7] R. Baldick, B. H. Kim, C. Chaseand, and Y. Luo. A fast distributed implementation of optimal power flow. *IEEE Trans. on Power Systems*, 14(3):858–863, 1999.

[8] B. H. Kim and R. Baldick. A comparison of distributed optimal power flow algorithms. *IEEE Trans. on Power Systems*, 15(2):599–604, 2000.

[9] J. A. Aguado and V. H. Quintana. Inter-utilities power-exchange coordination: a market-oriented approach. *IEEE Trans. on Power Systems*, 16(3):513–519, 2001.

[10] A. G. Bakirtzis and P. N. Biskas. A decentralized solution to the DC-OPF of interconnected power systems. *IEEE Trans. on Power Systems*, 18(3):1007–1013, 2003.

[11] P. N. Biskas, A. G. Bakirtzis, N. I. Macheras, and N. K. Pasialis. A decentralized implementation of DC optimal power flow on a network of computers. *IEEE Trans. on Power Systems*, 20(1):25–33, 2005.

[12] S. Lin and H. Chang. An efficient algorithm for solving BCOP and implementation. *IEEE Trans. on Power Systems*, 22(1):275–284, 2007.

[13] J. F. Bonnans. Mathematical study of very high voltage power networks I: The optimal DC power flow problem. *SIAM Journal on Optimization*, 7(4):979–990, 1997.

[14] S. H. Low. Convex relaxation of optimal power flow part I: Formulations and equivalence. *IEEE Trans. on Control of Network Systems*, 1(1):15–27, 2014.

[15] S. H. Low. Convex relaxation of optimal power flow part II: Exactness. *IEEE Trans. on Control of Network Systems*, to appear, 2014.

[16] S. Boyd and L. Vanderberghe. *Convex Optimization*. Cambridge University Press, 2004.

[17] J. Lavaei and S. H. Low. Zero duality gap in optimal power flow problem. *IEEE Trans. on Power Systems*, 27(1):92–107, 2012.

[18] S. Bose, D. F. Gayme, S. H. Low, and K. M. Chandy. Quadratically constrained quadratic programs on acyclic graphs with application to power flow. *arXiv:1203.5599*, 2012.

[19] J. Lavaei, A. Rantzer, and S. H. Low. Power flow optimization using positive quadratic programming. *Proc. of IFAC World Congress*, 2011.

[20] B. C. Lesieutre, D. K. Molzahn, A. R. Borden, and C. L. DeMarco. Examining the limits of the application of semidefinite programming to power flow problems. *2011 49th Annual Allerton Conference*, 2011.

[21] D. K. Molzahn, B. C. Lesieutre, and C. L. DeMarco. Investigation of non-zero duality gap solutions to a semidefinite relaxation of the optimal power flow problem. *2014 47th Hawaii International Conference on System Sciences (HICSS)*, 2014.

[22] R. A. Jabr. Radial distribution load flow using conic programming. *IEEE Trans. on Power Systems*, 21(3):1458–1459, 2006.

[23] S. Sojoudi and J. Lavaei. Physics of power networks makes hard optimization problems easy to solve. *Proc. of IEEE PES General Meeting*, 2012.

[24] L. Gan and S. H. Low. Optimal power flow in DC networks. *Proc. of IEEE Conference on Decision and Control (CDC)*, 2013.

[25] J. Lavaei, D. Tse, and B. Zhang. Geometry of power flows and optimization in distribution networks. *IEEE Trans. on Power Systems*, 29(2):572–583, 2014.

[26] X. Lou and C. W. Tan. Optimization decomposition of resistive power networks with energy storage. *IEEE Journal on Selected Areas in Communications*, to appear, 2014.

[27] M. Grant and S. Boyd. CVX: Matlab software for disciplined convex programming. *version 2.1, http://cvxr.com/cvx*, 2014.

[28] A. Simsek, A. E. Ozdaglar, and D. Acemoglu. Uniqueness of generalized equilibrium for box constrained problems and applications. *Proc. of Allerton*, 2005.

[29] A. Simsek, A. E. Ozdaglar, and D. Acemoglu. Generalized Poincare-Hopf theorem for compact nonsmooth regions. *Mathematics of Operations Research*, 32(1):193–214, 2007.

[30] D. P. Bertsekas. *Nonlinear Programming*. Athena Scientific, Belmont, MA, USA, 2nd edition, 2003.

[31] D. P. Bertsekas and J. N. Tsitsiklis. *Parallel and Distributed Computation: Numerical Methods*. Prentice Hall, NJ, 1989.

[32] J. D. Glover, M. S. Sarma, and T. J. Overbye. *Power System Analysis and Design*. Cengage Learning, 5th edition, 2011.

[33] Power System Test Case Archive. University of Washington, Seattle, WA. *Available: http://www.ee.washington.edu/research/*.

[34] R. D. Zimmerman, C. E. Murillo-Sánchez, and R. J. Thomas. MATPOWER's extensible optimal power flow architecture. *Proc. of IEEE PES General Meeting*, 2009.